



Effect of users height distribution on the coverage of mmwave cellular networks with 3d beamforming

Downloaded from: <https://research.chalmers.se>, 2023-05-05 16:56 UTC

Citation for the original published paper (version of record):

Baianifar, M., Razavizadeh, S., Khavari-Moghaddam, S. et al (2019). Effect of users height distribution on the coverage of mmwave cellular networks with 3d beamforming. IEEE Access, 7: 68091-68105. <http://dx.doi.org/10.1109/ACCESS.2019.2917509>

N.B. When citing this work, cite the original published paper.

©2019 IEEE. Personal use of this material is permitted.

However, permission to reprint/republish this material for advertising or promotional purposes

Received April 21, 2019, accepted May 13, 2019, date of publication May 17, 2019, date of current version June 6, 2019.

Digital Object Identifier 10.1109/ACCESS.2019.2917509

Effect of Users Height Distribution on the Coverage of mmWave Cellular Networks With 3D Beamforming

MAHDI BAIANIFAR¹, S. MOHAMMAD RAZAVIZADEH¹, (Senior Member, IEEE),
SOHEIL KHAVARI-MOGHADDAM¹, AND TOMMY SVENSSON²

¹School of Electrical Engineering, Iran University of Science and Technology (IUST), Tehran 16846-13114, Iran

²Department of Electrical Engineering, Chalmers University of Technology, SE-412 96 Gothenburg, Sweden

Corresponding author: S. Mohammad Razavizadeh (smrazavi@iust.ac.ir)

ABSTRACT In this paper, we study the effect of users' height distribution on the coverage probability of millimeter-wave (mmWave) cellular networks that utilize three-dimensional beamforming (3DBF). The users and base stations (BSs) are equipped with multiple antennas and both line-of-sight (LOS) and non-LOS links exist in the channel which are, respectively, modeled by the Nakagami- m and Rayleigh distribution. In this setup, we investigate the tilt angle optimization of the BS antenna arrays for maximizing the coverage probability under two regimes of *noise limited* and *interference limited*. In both cases, by adopting a stochastic geometry approach, we analytically derive the coverage probability, and then, find the optimal tilt angle that maximizes this probability. In addition, in the noise limited regime, we show that the optimal tilt angle depends on the average distance between each user and its serving BS and also their *effective height*. In the interference-limited regime, we further consider different rules for associating users to the BSs. Meanwhile, since in this regime, the tilt angle optimization is very complex, we propose a low complexity approach to find the optimal tilt angle that has a performance close to the optimal solution. We further study the asymptotic behavior when the density of the BSs or signal-to-interference ratio tends to infinity or zero. Finally, through the numerical simulations, we show that using the 3DBF and also incorporating the users' height distribution in the tilt angle optimization lead to a substantial improvement in the coverage probability of the mmWave cellular networks.

INDEX TERMS Stochastic geometry, mmWave networks, coverage probability, blockage, 3D beamforming, elevation beamforming, user height distribution.

I. INTRODUCTION

The constantly growing demand for high capacity and low latency communications has enforced many challenges to the design of next generation cellular networks. The fast increment in the number of connected devices and richer media content which must be delivered to user equipments anywhere and at any time have given significant importance to improving the network performance in terms of coverage and capacity [1], [2]. One of the potential techniques is three dimensional beamforming (3DBF) in which the main idea is to steer the radiation patterns to desired directions in 3D space and therefore increasing the signal power at the intended receivers and reducing interference [3], [4]. To this end, adjusting the elevation angle of the BS antenna pattern,

known as tilt angle, has the main role. This brings a significant improvement in the network performance compared to the conventional 2D beamforming (2DBF) methods which only steer the beams in the horizontal domain. In general this adjustment is not a trivial task due to complicated non-linear dependency of the performance metrics on the tilt angle [5], [6]. In practical scenarios, an active antenna system (AAS) is utilized to implement the 3DBF [3]. AAS provides us with the ability to adaptively steer the antenna array beam pattern electronically through controlling phase and amplitude of each antenna element signal [7]. This is a great potential candidate for addressing the adaptability demands in next generation cellular networks and self organizing networks (SON) solutions [8]. Tilt angle optimization via AAS, is one of the main candidates proposed for SON [9], [10]. Another promising technology for next generation wireless networks is millimeter wave (mmWave)

The associate editor coordinating the review of this manuscript and approving it for publication was Md. Arafatur Rahman.

systems. The mmWave frequency bands have many advantages including larger bandwidth, more frequency reuse and higher data rates [11], [12]. But, on the other hand, diverse range of absorption and path loss, make the mmWave networks prone to problems like the blockage effect which is caused by buildings and human bodies [2]. Owing to the shorter wavelength in the mmWave frequency bands, a larger number of antenna elements can be fitted in a reasonably sized array which gives more degrees of freedom in designing the 3DBF techniques. Meanwhile to investigate the performance of cellular networks, techniques based on stochastic geometry (SG) have attracted a lot of interests recently [13], [14]. Simplifying the analyses, providing lower bound of the network performance and modeling near to real scenarios are among the advantages of the SG approaches. The SG tool provides a useful and tractable paradigm for analyzing the performance metric of the network e.g. coverage probability, ergodic rate, and bit error rate probability [15].

In most of the previous works on 3DBF, height of the users are either ignored or assumed to be constant which are not consistent with real scenarios. In the practical scenarios, some of the users are indoor and the remaining are located in outdoors. In the case of the mmWave network, we cannot assume walls and floors shielding the communications, so rather indoor multi-level structures as shopping malls, exhibition centers and large hotel lobby areas with common open space covering several floors. Furthermore, the outdoor users in a more realistic model can experience different geographical height differences in urban area specially when they are located on elevated outdoor structures (e.g., bridges, staircases, and stadium). Although modeling the user positions on the ground and in a two dimensional (2D) coordinate system simplifies the analyses, the performance loss due to ignoring a practical 3D environment can be intolerable. In a practical 3D environment, height of the users should be modeled with a suitable random distribution.

Motivated by the above facts, in this paper we propose a mmWave network that utilizes 3DBF and then investigate the effect of the user height distribution on the coverage probability of this network. The tilt angle parameter of the AAS's employed in the BS's are controlled via a centralized control center and can be changed adaptively in response to network variations or users activities. We exploit a SG tool to mathematically analyze the coverage probability and then find the optimal tilt angle of the BS antenna arrays. We consider a mmWave cellular network in which the BSs are distributed according to a Poisson point process PPP in the x - y plane (on the ground) and they have fixed height in the z axis. The users are outdoor and randomly placed at different heights that are drawn from a probability distribution. In the environment both line of sight (LOS) and non-LOS (NLOS) propagation conditions exist and they are respectively modeled by Nakagami- m and Rayleigh distribution. In this setup we investigate the tilt angle optimization for maximizing the coverage probability under two regimes of noise limited and

interference limited systems. In both cases, by using tools from the SG approach, we analytically derive the coverage probability of the network and then find the optimal tilt angle that maximizes the coverage probability. We show that in the noise limited regime, the optimal tilt angle depends on the average distance of each user to its serving BS and also their *effective height*. In addition, in the interference limited regime, we further consider different rules for associating users to the BSs namely nearest BS (NBS), minimum path loss BS (MPLBS) and the strongest BS (SBS). In this regime, the tilt angle optimization is very complex and hence we propose a low complexity approach to find the optimal tilt angle and show that the proposed approach has a performance close to the optimal solution. We further study the asymptotic behavior of the coverage probability when the density of the BSs tends to infinity or zero and also when the signal to interference ratio tends to infinity or zero. Finally, through numerical simulations, we show that using the 3DBF and also including the users height distribution in the tilt angle optimization result in substantial improvements in the coverage performance of the mmWave cellular networks.

A. RELATED WORKS

The area spectral efficiency (ASE) and the coverage probability in the downlink transmission of ultra-dense small cell networks assuming constant height for the users and BSs is derived in [16]. Therein the *effective height* between the transmitter and receiver is assumed to be constant and multipath fading distribution for LOS paths is assumed to be Rician while the NLOS path propagation is assumed to be Rayleigh. In [17], temporal evaluation of the blocking effect by considering the effect of the users height in a simplified mmWave network is studied. In [18] the effect of base station (BS) antenna height and BS density on the coverage of a mmWave network is considered when the distribution of the LOS and NLOS propagation paths are different. The optimal density and height of BSs are obtained for some special cases. In [19] a multi-objective dynamic optimization is presented for maximizing the coverage of the network based on system cell site planning parameters (i.e. BS transmit power, antenna height, tilt angle). A common system model simplification in most of these works is the uniform isotropic antenna radiation pattern. On the other hand some other works do not consider an isotropic antenna radiation pattern and use the 3DBF to steer the radiation pattern in desired directions.

The impact of optimal tilt angle on the performance of the network is studied in [5], [6], [9], [20]–[24]. The tilt angle optimization is performed to either reduce the multi-cell interference or to maximize the desired signal power of users in a single cell. In [21], the problem of joint optimization of tilt angle and base station density in multi-tier networks is proposed. In [22], it is shown that a random placement of the users in the height domain affects the optimal tilt angle drastically. Authors in [23] investigate BS antenna downtilt adjusting for maximizing the coverage probability and area spectral efficiency. They consider the downlink of a cellular

network assuming that the BSs and the users are equipped with an antenna array which is modeled with a single antenna, capable of adjusting tilt angle. Also, sub-6GHz frequencies and constant effective height are assumed. Finally, in [24], the problem of maximizing the energy efficiency of mmWave cellular networks via tilt angle optimization is considered. Therein, the BSs and users are equipped with an antenna array and a simplified channel model is assumed. In this paper also, an uniform linear array and constant effective height are assumed.

B. CONTRIBUTIONS

Our main contributions are as follows:

- 1) Using a stochastic geometry approach, we study the effect of the BSs tilt angle on the coverage probability of the 3DBF enabled mmWave cellular networks. In addition, we find the optimal tilt angle that maximizes the coverage probability in the two regimes of noise limited and interference limited.
- 2) We consider the effect of users height on the coverage probability of the mmWave networks. For a general users height distribution, a closed-form expression for the coverage probability is derived. It is shown through numerical simulations that ignoring the users height distribution results in a significant performance degradation.
- 3) In the noise limited regime, a closed-form solution is derived for the optimal tilt angle when the height and distance of the users are fixed and known at the BS. In this case, the optimal tilt angle is abstained analytically as a function of the average distance between each user and its serving BS and also on their effective height. Furthermore, in a general case that the distance between the user and its serving BS and its effective height are random, we calculate an approximate tilt angle and show that it is very close to the optimal tilt angle. On the other hand, in the interference limited regime, we propose a low complexity approach for optimizing the tilt angle that performs very close to the optimal value.
- 4) Two different distributions for LOS and NLOS conditions are assumed in the environment. In addition, three different user association rules, namely the NBS, MPLBS and SBS are studied for deriving the coverage probability. In addition, we study the asymptotic behavior of the coverage probability when the density of the BSs and the signal to interference ratio tends to infinity or zero.

C. ORGANIZATION

The rest of the paper is organized as follows: In Sec. II, the system model is described. Sec. III presents the derivation of the coverage probability and its relation with the tilt angle and propose a low complexity approach for maximizing the coverage probability. In Sec. IV, asymptotic scenarios are presented. Sec. V illustrates the numerical results and finally Sec. VI concludes the paper.

II. SYSTEM MODEL

Consider the downlink of a mmWave cellular network in which BSs and users are equipped with N_t and N_r antennas, respectively. It is assumed that the location of the BSs is modeled as a homogeneous PPP, $\Phi \in \mathbb{R}^2$ with density λ_m , in which the location of the ℓ th BS is denoted by X_ℓ . Also, it is assumed that all of the BSs are active. To evaluate this network, we use the coverage probability as performance metric. For evaluating the performance of the network in the downlink, from the Slivnyak theorem, it is sufficient to only consider a typical user located at the origin [25]. We utilize antenna port approach for modeling the received signal at the BS antenna array as considered in [26], [27]. The channel matrix between the typical user and the ℓ th BS is denoted by $\mathbf{H}_\ell \in \mathbb{C}^{N_r \times N_t}$ and expressed as

$$\mathbf{H}_\ell = \sqrt{N_t N_r g_\ell} \sqrt{G(\theta_{\text{tilt}}, x_\ell, h_{\text{eff}})} L(x_\ell, h_{\text{eff}}) \mathbf{a}_r(\phi_\ell^r, \theta_\ell^r) \mathbf{a}_t^H(\phi_\ell^t, \theta_\ell^t), \quad (1)$$

where g_ℓ represents the small scale fading, where its amplitude in the case of LOS and NLOS links is assumed to be Nakagami- m and Rayleigh distributed, respectively. Also, $G(\theta_{\text{tilt}}, x_\ell, h_{\text{eff}})$ is the vertical antenna pattern gain of the ℓ th BS at the typical user as

$$G(\theta_{\text{tilt}}, x_\ell, h_{\text{eff}}) = 10^{-0.1 \min \left(12 \left(\frac{\theta_{\text{tilt}} - \arctan \frac{h_{\text{eff}}}{x_\ell}}{\theta_{3\text{dB}}} \right)^2, \text{SLL}_{\text{dB}} \right)}, \quad (2)$$

where as depicted in Fig. 1, θ_{tilt} denotes the BS antenna tilt angle, $h_{\text{eff}} = H_{\text{BS}} - H_u$ is the *effective height* (height difference between the typical user and the ℓ th BS). H_{BS} and H_u are the heights of the BSs and typical user, respectively. Also, x_ℓ denotes the horizontal distance between the typical user and its serving BS. Furthermore, SLL_{dB} and $\theta_{3\text{dB}}$ denote the side lobe level and 3dB beamwidth of the BS antenna pattern in the vertical domain. $L(x_\ell, h_{\text{eff}})$ in (1) denotes the path loss which is defined as

$$L(x_\ell, h_{\text{eff}}) = \begin{cases} (x_\ell^2 + h_{\text{eff}}^2)^{-\alpha_L/2} & \text{w.p. } P_L(x_\ell) \\ (x_\ell^2 + h_{\text{eff}}^2)^{-\alpha_N/2} & \text{w.p. } P_N(x_\ell) \end{cases}, \quad (3)$$

where $P_L(x_\ell)$ and $P_N(x_\ell) = 1 - P_L(x_\ell)$ denote the probability that a link is in LOS and NLOS condition, respectively and α_L and α_N denote the path loss exponent for these two conditions, respectively. Finally, $\phi_\ell^t(\theta_\ell^t)$ and $\phi_\ell^r(\theta_\ell^r)$ represent the physical angle of departure (AOD) and angle of arrival (AOA) in the horizontal (vertical) domain at the ℓ th BS and the typical user, respectively. Finally, $\mathbf{a}_t(\phi_\ell^t, \theta_\ell^t)$ and $\mathbf{a}_r(\phi_\ell^r, \theta_\ell^r)$ respectively denote the beam steering vector at the transmitter and receiver sides which for uniform planar arrays (UPAs) are obtained as follows [28]

$$\begin{aligned} \mathbf{a}_t(\phi_\ell^t, \theta_\ell^t) &= \frac{1}{\sqrt{N_t}} \left[1, \dots, e^{j2\pi \Delta_i (m \sin \phi_\ell^t \sin \theta_\ell^t + n \cos(\theta_\ell^t))}, \dots, \right. \\ &\quad \left. e^{j2\pi \Delta_i ((W-1) \sin \phi_\ell^t \sin \theta_\ell^t + (H-1) \cos(\theta_\ell^t))} \right]^T, \quad i \in \{t, r\}, \end{aligned} \quad (4)$$

where Δ_i , W_i and H_i are the normalized distance (to the wavelength) of the antenna elements at the transmitter/receiver side and number of the antenna elements at y and z axes, respectively. Antenna array size is $N_i = W_i H_i$.

As mentioned before, we assume that the height of the BS, H_{BS} , is fixed but the typical user can be located at different heights. In general, we assume that h_{eff} is distributed according to $f_{h_{\text{eff}}}(h)$ with support D_h .

It is assumed that each BS has an associated user and steers its beam to that user. Also, it is assumed that the typical user knows the AOA signal of its serving BS in the horizontal domain.

By the above assumptions, the ℓ th BS transmits a beam-formed signal $\mathbf{a}_\ell(\theta_\ell^t, \phi_\ell^t) s_\ell$, where s_ℓ denotes the data signal of the ℓ th BS to its user and $E\{s_\ell s_\ell^H\} = 1$. The typical user (which is denoted by index 0) multiplies its received signal by a decoding vector $\mathbf{a}_r^H(\theta_0^r, \phi_0^r)$ and the estimated signal \hat{s}_0 is

$$\begin{aligned} \hat{s}_0 &= \mathbf{a}_r^H(\theta_0^r, \phi_0^r) \mathbf{H}_0 \mathbf{a}_\ell(\theta_\ell^t, \phi_\ell^t) s_0 \\ &+ \sum_{\substack{\ell: X_\ell \in \Phi, \\ \ell \neq 0}} \mathbf{a}_r^H(\theta_0^r, \phi_0^r) \mathbf{H}_\ell \mathbf{a}_\ell(\theta_\ell^t, \phi_\ell^t) s_\ell + \mathbf{a}_r^H(\theta_0^r, \phi_0^r) \mathbf{n}, \end{aligned} \quad (5)$$

where $\phi_\ell^{t'}$ ($\theta_\ell^{t'}$) denotes the AOD of the ℓ th BS to its associated user in the horizontal (vertical) domain and $\mathbf{n} \sim \mathcal{CN}(0, \sigma^2)$ is the received noise at the typical user. Hence, the SINR at the typical user can be written as

$$\text{SINR} = \frac{|\mathbf{a}_r^H(\theta_0^r, \phi_0^r) \mathbf{H}_0 \mathbf{a}_\ell(\theta_\ell^t, \phi_\ell^t)|^2}{\sigma^2 + \sum_{\substack{\ell: X_\ell \in \Phi, \\ \ell \neq 0}} |\mathbf{a}_r^H(\theta_0^r, \phi_0^r) \mathbf{H}_\ell \mathbf{a}_\ell(\theta_\ell^t, \phi_\ell^t)|^2}. \quad (6)$$

Because of the array structure at the transmitter and receiver, we have

$$\begin{aligned} \mathbf{a}_i^H(\theta_\ell^i, \phi_\ell^i) \mathbf{a}_i(\theta_{\ell'}^i, \phi_{\ell'}^i) &= e^{j\pi \Delta_i (A(W_i-1) + B(H_i-1))} \\ &\times \frac{1}{N_i} \frac{\sin(\pi \Delta_i A W_i)}{\sin(\pi \Delta_i A)} \frac{\sin(\pi \Delta_i B H_i)}{\sin(\pi \Delta_i B)}, \end{aligned} \quad (7)$$

where $A = \sin \phi_\ell^i \sin \theta_\ell^i - \sin \phi_{\ell'}^i \sin \theta_{\ell'}^i$ and $B = \cos \theta_\ell^i - \cos \theta_{\ell'}^i$. For simplicity of formulation we define

$$\Lambda(Z_i^{\ell, \ell'}) = |\mathbf{a}_i^H(\theta_\ell^i, \phi_\ell^i) \mathbf{a}_i(\theta_{\ell'}^i, \phi_{\ell'}^i)|. \quad (8)$$

It is obvious from (8) that $\Lambda(Z_i^{\ell, \ell}) = 1$ for $i \in \{t, r\}$. Thus we can rewrite the SINR expression in (6) as follows

$$\text{SINR} = \frac{|g_0|^2 G(\theta_{\text{tilt}}, x_0, h_{\text{eff}}) L(x_0, h_{\text{eff}})}{\sigma_{\text{eff}}^2 + I}, \quad (9)$$

where

$$I = \sum_{\substack{\ell: X_\ell \in \Phi, \\ \ell \neq 0}} |g_\ell|^2 \Lambda^2(Z_r^{0, \ell}) G(\theta_{\text{tilt}}, x_\ell, h_{\text{eff}}) L(x_\ell, h_{\text{eff}}) \Lambda^2(Z_t^{\ell, \ell'}),$$

and $\sigma_{\text{eff}}^2 = \frac{\sigma^2}{N_t N_r}$. Using the above SINR, we derive the coverage probability in the noise limited and interference limited regimes, as described in the next section.

III. COVERAGE PROBABILITY

In this section, we derive the coverage probability for the two regimes of noise limited and interference limited systems. In these two regimes the SINR is reduced to signal to noise ratio (SNR) and signal to interference ratio (SIR), respectively. As mentioned before, we consider three different user association rules, namely the NBS, the MPLBS and the SBS. The coverage probability for the noise limited and interference limited regimes are defined as $P_{CN} = \Pr\{\text{SNR} \geq \tau\}$ and $P_{CI} = \Pr\{\text{SIR} \geq \tau\}$, respectively. Here, τ denotes the SNR or SIR threshold.

A. NOISE LIMITED REGIME

In this case, by setting $I = 0$ in (9) the coverage probability is calculated as follows

$$\begin{aligned} P_{CN} &= \Pr\{\text{SNR} \geq \tau\} \\ &= E_{x,h} \left\{ \Pr \left\{ |g_0|^2 G(\theta_{\text{tilt}}, x_0, h_{\text{eff}}) L(x_0, h_{\text{eff}}) > \tau_{\text{eff}} \right\} \right. \\ &\quad \left. x_0 = x, h_{\text{eff}} = h \right\} \\ &= E_{x,h} \left\{ P_L(x) \bar{F}_L \left(\frac{\tau_{\text{eff}} (x^2 + h^2)^{\frac{\alpha_L}{2}}}{N_t N_r G(\theta_{\text{tilt}}, x, h)} \right) \right\} \\ &\quad + E_{x,h} \left\{ P_N(x) \bar{F}_N \left(\frac{\tau_{\text{eff}} (x^2 + h^2)^{\frac{\alpha_N}{2}}}{N_t N_r G(\theta_{\text{tilt}}, x, h)} \right) \right\}. \end{aligned} \quad (10)$$

where $\tau_{\text{eff}} = \sigma_{\text{eff}}^2 \tau$ and $\bar{F}_L(y)$ and $\bar{F}_N(y)$ denote the power gain complementary cumulative distribution function (CCDF) of LOS and NLOS links, respectively, and are given by

$$\bar{F}_L(y) = e^{-my} \sum_{k=0}^{m-1} \frac{(my)^k}{k!}, \quad (11)$$

$$\bar{F}_N(y) = e^{-y}. \quad (12)$$

As seen, the coverage probability depends on the tilt angle and hence it can be improved by proper adjustment of this angle. The following lemma gives us an insight about the optimal tilt angle in this regime.

Lemma 1: *In the case that height and distance of the user are fixed and known at the BS, the optimal tilt angle is to the direction of the line connecting the typical user to its serving BS and is independent of the blockage and parameters of the channel fading.*

Proof: As seen from equation (10), the SNR coverage probability by assuming the distance and height of the user are fixed and known at its serving BS will be

$$\begin{aligned} P_{CN} &= P_L(x) \bar{F}_L \left(\frac{\tau_{\text{eff}} (x^2 + h^2)^{\frac{\alpha_L}{2}}}{N_t N_r G(\theta_{\text{tilt}}, x, h)} \right) \\ &\quad + P_N(x) \bar{F}_N \left(\frac{\tau_{\text{eff}} (x^2 + h^2)^{\frac{\alpha_N}{2}}}{N_t N_r G(\theta_{\text{tilt}}, x, h)} \right). \end{aligned}$$

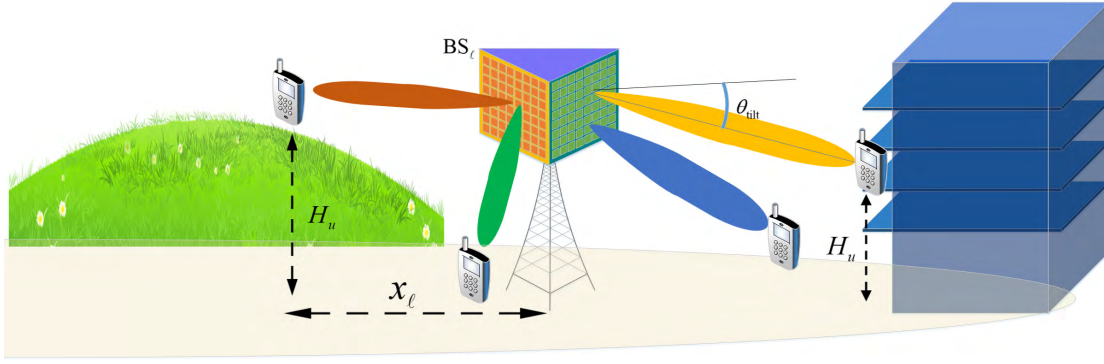


FIGURE 1. Network model and illustration of the system parameters.

By taking the derivative with respect to θ_{tilt} and defining $\kappa_L = \tau_{\text{eff}} (x^2 + h^2)^{\frac{\alpha_L}{2}}$, $\kappa_N = \tau_{\text{eff}} (x^2 + h^2)^{\frac{\alpha_N}{2}}$ and $G^{-1} = \frac{1}{G(\theta_{\text{tilt}}, x, h)}$ we have

$$\begin{aligned} \frac{dP_{CN}}{d\theta_{\text{tilt}}} &= P_L(x) e^{-m\kappa_L G^{-1}} \left[-m\kappa_L \sum_{i=0}^{m-1} \frac{(m\kappa_L G^{-1})^i}{i!} \right. \\ &\quad \left. + \sum_{i=0}^{m-1} \frac{i(m\kappa_L)^i (G^{-1})^{i-1}}{i!} \right] \frac{dG^{-1}}{d\theta_{\text{tilt}}} \\ &\quad - \kappa_N P_N(x) e^{-\kappa_N G^{-1}} \frac{dG^{-1}}{d\theta_{\text{tilt}}}. \end{aligned} \quad (13)$$

By setting $\frac{dP_{CN}}{d\theta_{\text{tilt}}} = 0$ and some manipulations, we have

$$\begin{aligned} &\left[\underbrace{-m\kappa_L P_L(x) e^{-m\kappa_L G^{-1}} \frac{(m\kappa_L G^{-1})^{m-1}}{(m-1)!} - \kappa_N P_N(x) e^{-\kappa_N G^{-1}}}_{\neq 0} \right] \\ &\quad \times \frac{dG^{-1}}{d\theta_{\text{tilt}}} = 0. \end{aligned} \quad (14)$$

Therefore to find θ_{tilt} , we need $\frac{dG^{-1}}{d\theta_{\text{tilt}}} = 0$. Notice that

$$\begin{aligned} G^{-1} &= e^{C_0 \left(\frac{\theta_{\text{tilt}} - \text{atan} \frac{h}{x}}{\theta_{3\text{dB}}} \right)^2} (U(\theta_{\text{tilt}} - f_2) - U(\theta_{\text{tilt}} - f_1)) \\ &\quad + e^{C_0 \text{SLL}_{\text{dB}}} (U(\theta_{\text{tilt}} - f_1) + U(-\theta_{\text{tilt}} + f_2)), \end{aligned} \quad (15)$$

where $U(\cdot)$ represents the unit step function, $C_0 = 1.2 \log 10$, $f_1 = \text{atan} \frac{h}{x} + \theta_{3\text{dB}} \sqrt{\frac{\text{SLL}_{\text{dB}}}{12}}$ and $f_2 = \text{atan} \frac{h}{x} - \theta_{3\text{dB}} \sqrt{\frac{\text{SLL}_{\text{dB}}}{12}}$. Hence, by taking derivative with respect to θ_{tilt} , we have

$$\begin{aligned} \frac{dG^{-1}}{d\theta_{\text{tilt}}} &= 2C_0 \left(\frac{\theta_{\text{tilt}} - \text{atan} \frac{h}{x}}{\theta_{3\text{dB}}} \right) e^{C_0 \left(\frac{\theta_{\text{tilt}} - \text{atan} \frac{h}{x}}{\theta_{3\text{dB}}} \right)^2} \\ &\quad \times (U(\theta_{\text{tilt}} - f_2) - U(\theta_{\text{tilt}} - f_1)). \end{aligned} \quad (16)$$

Consequently, it is seen from (16) that the optimal tilt angle is $\theta_{\text{tilt}} = \text{atan} \frac{h}{x}$ which is to the direction of the line connecting the typical user to its serving BS. ■

In general, distance between the typical user and its serving BS and the *effective height* are random. However, in the following lemma, we show that an approximated tilt angle can be found by using statistical average. By numerical results, we show that this approximated tilt angle is close to the optimal tilt angle found by the exhaustive search.

Lemma 2: *In the noise limited regime, when the user's distances and effective height are random, the optimal tilt angle can be approximated by $\theta_{\text{tilt}} \approx \text{atan} \frac{\bar{h}}{\bar{x}}$, where $\bar{h} = E_{h_{\text{eff}}} \{h\}$ and $\bar{x} = E_x \{x\}$.*

Proof: By taking derivative with respect to θ_{tilt} from (10) we have

$$\begin{aligned} \frac{dP_{CN}}{d\theta_{\text{tilt}}} &= E_{r,h} \left\{ \left[-m\kappa_L P_L(r) e^{-m\kappa_L G^{-1}} \frac{(m\kappa_L G^{-1})^{m-1}}{(m-1)!} \right. \right. \\ &\quad \left. \left. - \kappa_N P_N(r) e^{-\kappa_N G^{-1}} \right] \frac{d}{d\theta_{\text{tilt}}} G^{-1} \right\} = E_{r,h} \{ \mathcal{K}(r, h) \} \end{aligned} \quad (17)$$

By using Taylor series expansion around $\bar{r} = E\{r\}$, $\bar{h} = E\{h\}$, we have

$$\mathcal{K}(r, h) \approx \mathcal{K}(\bar{r}, \bar{h}) + \mathcal{K}'_r(\bar{r}, \bar{h})(r - \bar{r}) + \mathcal{K}'_h(\bar{r}, \bar{h})(h - \bar{h}), \quad (18)$$

where \mathcal{K}'_i , $i \in \{r, h\}$ denotes the derivative with respect to variable i . By substituting (18) in (17), we have $\frac{dP_{CN}}{d\theta_{\text{tilt}}} = \mathcal{K}(\bar{r}, \bar{h})$. By setting $\mathcal{K}(\bar{r}, \bar{h}) = 0$ and using the result of lemma 1, the proof is completed. ■

B. INTERFERENCE LIMITED REGIME

By setting $\sigma_{\text{eff}}^2 = 0$ in (9) the coverage probability in the interference limited regime is calculated as $P_{C^I} = \Pr \{ \text{SIR} > \tau \}$. In this regime, we consider three different user association rules and in the following we derive the coverage probability for each of them.

1) NBS ASSOCIATION RULE

In this case, the typical user is associated with its nearest BS. By defining the probability distribution of the distance R

between the typical user and its associated BS as $f_R^{NB}(x) = 2\pi\lambda_m x e^{-\pi\lambda_m x^2}$, the coverage probability is obtained from the following theorem.

Theorem 1: In the mmWave cellular networks, by considering the 3DBF and users height distribution, using the NBS user association rule, the coverage probability is obtained as

$$P_{CI} = \int_0^\infty \int_{D_h} \left\{ P_L(r) \sum_{k=0}^{m-1} \frac{(-ms_L)^k}{k!} \left[\frac{d^k}{dz^k} \mathcal{L}_I(z) \right]_{z=ms_L} \right. \\ \left. + P_N(r) \mathcal{L}_I(s_N) \right\} f_{h_{eff}}(h) f_R^{NB}(r) dh, \quad (19)$$

where $s_L = \frac{\tau(r^2+h^2)^{\frac{\alpha_L}{2}}}{G(\theta_{tilt}, r, h)}$ and $s_N = \frac{\tau(r^2+h^2)^{\frac{\alpha_N}{2}}}{G(\theta_{tilt}, r, h)}$. $\mathcal{L}_I(z)$ represents the Laplace functional of the interference which is given as follows

$$\mathcal{L}_I(z) = \exp \left(-2\pi\lambda_m \int_r^\infty (1 - E_{Z_t, Z_r} \{K_L(Z_t, Z_r, m, \theta_{tilt}, x, h)\}) x P_L(x) dx \right) \\ \times \exp \left(-2\pi\lambda_m \int_r^\infty (1 - E_{Z_t, Z_r} \{K_N(Z_t, Z_r, 1, \theta_{tilt}, x, h)\}) x P_N(x) dx \right), \quad (20)$$

where

$$K_w(Z_t, Z_r, m, \theta_{tilt}, x, h) = \frac{1}{\left(1 + \frac{z}{m} \Lambda^2(Z_r) G(\theta_{tilt}, x, h) (x^2 + h^2)^{-\frac{\alpha_w}{2}} \Lambda^2(Z_t)\right)^m}, \\ w \in \{L, N\}, \quad (21)$$

where superscripts of Z_r and Z_t are omitted for simplicity.

Proof: Please refer to Appendix VI for the proof. ■

In calculation of $E_{Z_t, Z_r} \{K_w(Z_t, Z_r, m, \theta_{tilt}, x, h)\}$, we can use a discrete binary model. In this approach, we can assume binary interference where according to (4) we have

$$\Lambda(Z_i^{\ell, \ell'}) = \begin{cases} 1 & \text{with probability } \frac{1}{N_i} \\ 0 & \text{with probability } 1 - \frac{1}{N_i} \end{cases}. \quad (22)$$

Therefore, in this case we have

$$\mathcal{L}_{L_L}(z) = \exp \left(-2\pi C_1 \lambda_m \int_r^\infty \frac{1}{\left(1 + \frac{z}{m} G(\theta_{tilt}, x, h) (x^2 + h^2)^{-\alpha_L/2}\right)^m} x P_L(x) dx \right) \\ \times \left(1 - \frac{1}{\left(1 + \frac{z}{m} G(\theta_{tilt}, x, h) (x^2 + h^2)^{-\alpha_L/2}\right)^m} \right) x P_L(x) dx \quad (23)$$

$$\mathcal{L}_{L_N}(z) = \exp \left(-2\pi C_1 \lambda_m \int_r^\infty \frac{x P_N(x) dx}{1 + \frac{(x^2 + h^2)^{\alpha_N/2}}{z G(\theta_{tilt}, x, h)}} \right). \quad (24)$$

where $C_1 = \frac{1}{N_t N_r}$.

2) MPLBS ASSOCIATION RULE

In this case, the typical user is associated with the BS that provides the minimum path loss. The following lemma gives the probability for the typical user to be associated with a LOS and NLOS BS.

Lemma 3: By considering the users height distribution and the minimum path loss criteria, the probability for the typical user to be associated with LOS and NLOS BS, which are denoted by \mathcal{A}_L and \mathcal{A}_N , respectively, can be derived as

$$\mathcal{A}_L = \int_{D_h} \int_0^\infty \exp \left(-2\pi\lambda_m \int_0^{\gamma(r, h)} x P_N(x) dx \right) \\ \times f_{r_L}(r) f_{h_{eff}}(h) dr dh, \quad (25)$$

where $\gamma(r, h) = \sqrt{\max \left((r^2 + h^2)^{\frac{\alpha_L}{\alpha_N}} - h^2, 0 \right)}$ and $f_{r_L}(r) = 2\pi\lambda_m P_L(r) e^{-2\pi\lambda_m \int_0^r x P_L(x) dx}$ and $\mathcal{A}_N = 1 - \mathcal{A}_L$.

Proof: The typical user connects to a LOS BS if the path loss of the NBS in Φ_L is smaller than that of the NBS in Φ_N . Therefore

$$\mathcal{A}_L = \Pr \left\{ (r_L^2 + h^2)^{-\frac{\alpha_L}{2}} > (r_N^2 + h^2)^{-\frac{\alpha_N}{2}} \right\} \\ = E_h \left\{ \int_0^\infty \Pr \left\{ r_N > \sqrt{(r^2 + h^2)^{\frac{\alpha_L}{\alpha_N}} - h^2} \mid r_L = r \right\} \right. \\ \left. f_{r_L}(r) dr \right\}, \quad (26)$$

where by using the null probability of a PPP, we have $\Pr \{r_N > \gamma\} = \exp(-2\pi\lambda_m \int_0^\gamma x P_N(x) dx)$ [29]. Also, for calculating $f_{r_L}(r)$ we use the fact that $f_{r_L}(r) = \frac{d}{dr} (1 - \Pr \{r_L > r\})$. ■

We denote the distance of the typical user to its LOS and NLOS BS by R^L and R^N , and their probability density function (PDF) by $f_L(r)$ and $f_N(r)$, respectively, which are given by the following lemma.

Lemma 4: The PDF for the distance of the typical user to its serving LOS and NLOS BS by considering the MPLBS user association rule are respectively given by

$$f_L(r) = \frac{f_{r_L}(r)}{\mathcal{A}_L} \int_{D_{h_{eff}}} \exp \left(-2\pi\lambda_m \int_0^{\gamma(r, h)} x P_N(x) dx \right) f_{h_{eff}}(h) dh \quad (27)$$

$$f_N(r) = \frac{f_{r_N}(r)}{\mathcal{A}_N} \int_{D_{h_{eff}}} \exp \left(-2\pi\lambda_m \int_0^{\zeta(r, h)} x P_L(x) dx \right) f_{h_{eff}}(h) dh, \quad (28)$$

where $\zeta(r, h) = \sqrt{(r^2 + h^2)^{\frac{\alpha_N}{\alpha_L}} - h^2}$ and $f_{r_N}(r) = 2\pi\lambda_m P_N(r) e^{-2\pi\lambda_m \int_0^r x P_N(x) dx}$.

Proof: If we denote the event that the typical user is connected to the LOS BS by E^L , we have

$$\Pr\{R^L > r\} = \Pr\{r_L > r | E^L\} = \frac{\Pr\{r_L > r \cap E^L\}}{A_L}, \text{ where}$$

$$\Pr\{r_L > r \cap E^L\} = \int_r^\infty \Pr\left\{\left(r_L^2 + h^2\right)^{-\frac{\alpha_L}{2}} > \left(r_N^2 + h^2\right)^{-\frac{\alpha_N}{2}} \middle| r_L = x\right\} f_{r_L}(x) dx, \quad (29)$$

where by using lemma 3 and using the fact that $f_L(r) = -\frac{d}{dr} \Pr\{R^L > r\}$ the proof is completed. A similar approach can be used for calculating $f_N(r)$. ■

In the following we derive the coverage probability by using the minimum path loss user association rule.

Theorem 2: In the mmWave cellular networks, by considering 3DBF and users height distribution, and by using the MPLBS user association rule, the coverage probability is given by

$$P_{C^I} = A_L P_c^L + A_N P_c^N, \quad (30)$$

where P_c^L is

$$P_c^L = \int_0^\infty \int_{D_{h_{\text{eff}}}} E_I\{\bar{F}_L(s_L I)\} f_{h_{\text{eff}}}(h) f_L(r) dh dr, \quad (31)$$

and in which $E_I\{\bar{F}_L(\cdot)\}$ can be calculated using (48). In addition, $\mathcal{L}_I(z) = \mathcal{L}_{I_L}(z) \mathcal{L}_{I_N}(z)$, where $\mathcal{L}_{I_L}(z)$ is given by (49) and $\mathcal{L}_{I_N}(z)$ is given by

$$\mathcal{L}_{I_N}(z) = \exp\left(-2\pi\lambda_m \int_{\gamma(r,h)}^\infty \left(1 - E_{Z_t, Z_r}\{K_N(Z_t, Z_r, 1, \theta_{\text{tilt}}, x, h)\}\right) x P_N(x) dx\right). \quad (32)$$

Also, we have

$$P_c^N = \int_0^\infty \int_{D_{h_{\text{eff}}}} E_I\{\bar{F}_N(s_N I)\} f_{h_{\text{eff}}}(h) f_N(r) dh dr, \quad (33)$$

where $E_I\{\bar{F}_N(s_N I)\} = \mathcal{L}_I(s_N)$. Furthermore, in this case $\mathcal{L}_I(z) = \mathcal{L}_{I_L}(z) \mathcal{L}_{I_N}(z)$, where we have

$$\mathcal{L}_{I_L}(z) = \exp\left(-2\pi\lambda_m \int_{\zeta(r,h)}^\infty \left(1 - E_{Z_t, Z_r}\{K_L(Z_t, Z_r, \theta_{\text{tilt}}, m, x, h)\}\right) x P_L(x) dx\right), \quad (34)$$

and $\mathcal{L}_{I_N}(z)$ is given by (50).

Proof: Proof is similar to the theorem 1 and is omitted here. ■

3) SBS ASSOCIATION RULE

The following theorem provides the coverage probability for the SBS user association rule.

Theorem 3: In the mmWave network, by considering 3DBF and users height distribution, and by using the SBS user association rule, the coverage probability is

$$P_{C^I} = 2\pi\lambda_m \int_0^\infty \int_{D_h} \left\{ \sum_{k=0}^{m-1} \frac{(-ms_L)^k}{k!} \left[\frac{d^k}{dz^k} \mathcal{L}_I(z) \right]_{z=ms_L} \times P_L(r) + \mathcal{L}_I(s_N) P_N(r) \right\} f_{h_{\text{eff}}}(h) r dh dr, \quad (35)$$

where $\mathcal{L}_I(z) = \mathcal{L}_{I_L}(z) \mathcal{L}_{I_N}(z)$ is given as follows.

$$\mathcal{L}_{I_L}(z) = \exp\left(-2\pi\lambda_m \int_0^\infty \left(1 - E_{Z_t, Z_r}\{K_L(Z_t, Z_r, m, \theta_{\text{tilt}}, x, h)\}\right) x P_L(x) dx\right) \quad (36)$$

$$\mathcal{L}_{I_N}(z) = \exp\left(-2\pi\lambda_m \int_0^\infty \left(1 - E_{Z_t, Z_r}\{K_N(Z_t, Z_r, 1, \theta_{\text{tilt}}, x, h)\}\right) x P_N(x) dx\right). \quad (37)$$

Proof: Please refer to Appendix VI for the proof. ■

In the noise limited regime, we provided an approximated optimal tilt angle for maximizing the coverage probability. However, in the interference limited regime, to optimize the coverage probability, for each value of θ_{tilt} , equations (19), (30) and (3) are evaluated which are complicated functions of θ_{tilt} . For reducing the complexity of the calculations, we propose a low complexity approach for finding the optimal value of the tilt angle. Considering the NBS association rule and the PDF of the distance between the typical user and its serving BS, i.e. $f_R^{NB}(r)$, it is sufficient to consider ranges of r such that $\int_{r_0}^{r_1} f_R^{NB}(r) dr \geq 1 - \epsilon$. It results in the interval $r_0 \leq r \leq r_1$ where $r_0 = \sqrt{\frac{-\ln \frac{\epsilon}{2}}{\pi\lambda_m}}$ and $r_1 = \sqrt{\frac{-\ln(1-\frac{\epsilon}{2})}{\pi\lambda}}$. By considering this fact, the optimum tilt angle lies in the following interval

$$\max\left(\text{atan}\left(\frac{h_{\min}}{r_1}\right) - \theta_{3\text{dB}} \sqrt{\text{SLL}_{\text{dB}}/12}, 0\right) \leq \theta_{\text{tilt}} \leq \text{atan}\frac{h_{\max}}{r_0} + \theta_{3\text{dB}} \sqrt{\text{SLL}_{\text{dB}}/12},$$

where h_{\min} and h_{\max} denote the minimum and maximum effective height between the typical user and its serving BS. An interesting observation is that for small values of λ_m , r_0 and r_1 are large and consequently, the length of the interval containing optimal tilt angle decreases. For example if we consider $\theta_{3\text{dB}} = 6^\circ$, $\text{SLL}_{\text{dB}} = 20\text{dB}$, $\lambda_m = 10^{-6}$ and $\epsilon = 0.1$, then we have $r_0 = 127.78$ and $r_1 = 976.7$, which results in $0^\circ \leq \theta_{\text{opt}} \leq 9^\circ$. However, the length of the interval containing the optimal tilt angle θ_{tilt} for moderate values of λ_m will be large. In the following we propose a low complexity approach for finding the optimal value of the tilt angle based on the above mentioned fact, i.e., we use the Taylor series expansion of the coverage probability around $\bar{r} = \frac{1}{2\sqrt{\lambda_m}}$ (resulted from the NBS user association rule) and $\bar{h} = \int_{D_h} h f_h(h) dh$ in conjunction with the Bisection method. Algorithm 1 summarizes the proposed low complexity approach where we define

$$\theta_{\min} = \max\left(\text{atan}\left(\frac{\bar{h}}{\bar{r}}\right) - \theta_{3\text{dB}} \sqrt{\text{SLL}_{\text{dB}}/12}, 0\right) \quad (38)$$

$$\theta_{\max} = \text{atan}\left(\frac{\bar{h}}{\bar{r}}\right) + \theta_{3\text{dB}} \sqrt{\text{SLL}_{\text{dB}}/12} \quad (39)$$

Algorithm 1 Proposed Low Complexity Approach

- 1: Initialize $\theta_{\text{tilt}}^{\min} = \theta_{\min}$ and $\theta_{\text{tilt}}^{\max} = \theta_{\max}$ and calculate the coverage probability for these values of θ_{tilt} .
- 2: Calculate the coverage probability for $\theta_{\text{tilt}} = \frac{\theta_{\text{tilt}}^{\min} + \theta_{\text{tilt}}^{\max}}{2}$.
- 3: If the resulted coverage probability is larger than the result for $\theta_{\text{tilt}}^{\min}$, then set $\theta_{\text{tilt}}^{\min} = \theta_{\text{tilt}}$. Otherwise set $\theta_{\text{tilt}}^{\max} = \theta_{\text{tilt}}$.
- 4: Stop when $|\theta_{\text{tilt}}^{\min} - \theta_{\text{tilt}}^{\max}|$ is less than a predefined value.

Notice that the proposed low complexity approach can be used in the noise limited regime too. Also, using a similar approach as in the noise limited regimes, we can use Taylor expansion to obtain an approximate value for the optimal tilt angle where we have

$$\theta_{\text{opt}} \approx \text{atan}\left(\frac{\bar{h}}{\bar{r}}\right), \quad (40)$$

where it is equal to the result obtained for the noise limited regime given by lemma 2. We show that the performance of the proposed low complexity approach is very close to the optimal solution found by the exhaustive search for the corresponding user association rules.

IV. ASYMPTOTIC SCENARIOS

In this section, we consider the case when the BSs density goes to infinity or vanishes to zero. It is obvious that when λ_m goes to infinity the coverage probability of the network is P_c^L , since all the BSs have LOS with the typical user. In the following lemma we prove that despite increasing the density of the BSs, the coverage probability tends to zero.

Lemma 5: In mmWave cellular networks with 3DBF, when the BS density tends to infinity, the coverage probability tends to zero.

Proof: Please refer to Appendix VI for the proof. ■

Before stating the theorem for the case that $\lambda_m \rightarrow 0$, it is useful to note that for the nearest and strongest BS user association rules we have, respectively

$$P_{C^I}^{NBS} = E_{h,r} \left\{ \exp \left(-2\pi C_1 \lambda_m \int_r^\infty \frac{xdx}{1 + \frac{G(\theta,r,h)(x^2+h^2)^{\frac{\alpha_N}{2}}}{\tau G(\theta,x,h)(r^2+h^2)^{\frac{\alpha_N}{2}}}} \right) \right\} \quad (41)$$

$$P_{C^I}^{SBS} = E_{h,r} \left\{ \exp \left(-2\pi C_1 \lambda_m \int_0^\infty \frac{xdx}{1 + \frac{G(\theta,r,h)(x^2+h^2)^{\frac{\alpha_N}{2}}}{\tau G(\theta,x,h)(r^2+h^2)^{\frac{\alpha_N}{2}}}} \right) \right\}. \quad (42)$$

Lemma 6: In mmWave cellular networks, when the BS density and the SIR threshold tend to zero, for the nearest and

strongest BS user association rules, respectively we have

$$1 - P_c^{NBS} \approx \frac{4\pi C_1 \lambda_m}{\alpha_N - 2} E_{h,r} \left\{ (r^2 + h^2) G^{-1}(\theta, r, h) \right\} \tau$$

$$1 - P_c^{SBS} \approx \frac{2\pi^2 C_1 \lambda_m}{\sin\left(\frac{2\pi}{\alpha_N}\right)} E_{h,r} \left\{ (r^2 + h^2) G^{-\frac{2}{\alpha_N}}(\theta, r, h) \right\} \tau^{\frac{2}{\alpha_N}}$$

Proof: Please refer to Appendix VI for the proof. ■

The following lemma investigates the behavior of the coverage probability when $\tau \rightarrow \infty$, $\lambda_m \rightarrow 0$.

Lemma 7: In the mmWave cellular networks, when the BS density tends toward zero and the SIR threshold tends to infinity, for the nearest and strongest BS user association rules, respectively we have

$$P_{C^I}^{NBS} \approx \frac{G_{\min}^{-\frac{4}{\alpha_N}}}{C_2^2} E_h \left\{ \frac{1}{\pi C_1 \lambda_m h^2} \right\} \tau^{-\frac{4}{\alpha_N}} \quad (43)$$

$$P_{C^I}^{SBS} \approx \frac{\sin\left(\frac{2\pi}{\alpha_N}\right)^2}{2\pi^3 C_1 \lambda_m} E_h \left\{ \frac{1}{h^2} \right\} \tau^{-\frac{4}{\alpha_N}}, \quad (44)$$

$$\text{where } C_2 = \left(\frac{\Gamma\left(1 - \frac{2}{\alpha_N}\right)}{\Gamma\left(1 - \frac{4}{\alpha_N}\right)} \right)^2.$$

Proof: Please refer to Appendix VI for the proof. ■

V. NUMERICAL RESULTS

In this section, we numerically evaluate the performance of the proposed 3DBF method in the mmWave networks and analyze the effect of the users height on the performance. In order to model users height distribution, the 3GPP specifications have proposed a discrete model for height distribution that models the user's placement on the building floors [32] which is suitable for modeling the indoor users. To model the users height distribution of outdoor users, a more suitable model is introduced in [7]. In this paper, we consider a more general model which is based on the models in [7] and [32], which takes the majority of the users placed in a specific height into account [22]

$$f_{h_{\text{eff}}}(h) = a \delta(h - h_0) + (1 - a)(b h + c), \quad (45)$$

where $0 \leq a \leq 1$ denotes the fraction of the users located at height h_0 and b and c are two constants depending on the environment and the height of the users. We use $P_L(r) = e^{-\beta r}$ where β is the blockage parameter [30]. For the BSs and user height, we use the typical values mentioned at [28]. Also, range of the tilt angle is assumed to vary in the interval 0° and 90° [6], [20] and the tilt angle variation step assumed to be 1° [31].

First, we study the coverage probability in the noise limited regime and assess the correctness of the lemmas 1 and 2. Fig. 2, represents the coverage probability versus the tilt angle for different values of β and h_{eff} with $\lambda_m = 10^{-5}$ (we consider $\lambda_m \leq 10^{-5}$ as the noise limited regime and the BSs density larger than this threshold as the interference limited regime). As it is seen, the optimal tilt angle equals to

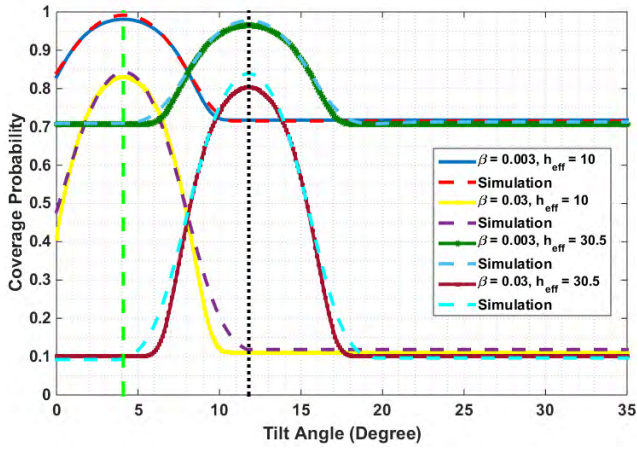


FIGURE 2. Coverage probability versus the tilt angle in the noise limited regime for different values of β and h_{eff} (for $x = 150$).

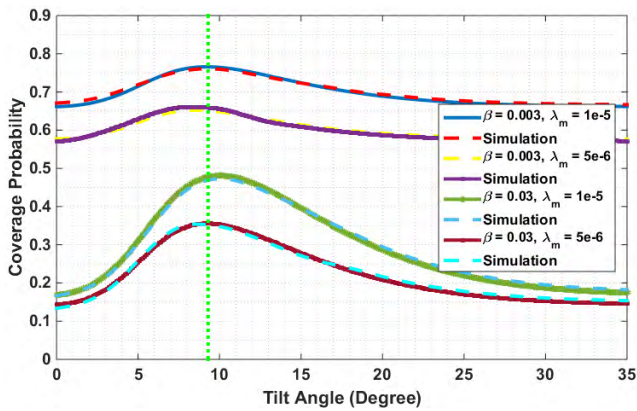


FIGURE 3. Coverage probability versus tilt angle in the noise limited regime for different values of β and λ_m .

the horizontal angle between the typical user and its serving BS. This angle is not related to other network parameters as was proved before in the lemma 1. In this figure, the vertical lines show the optimal tilt angle obtained by lemma 1.

Also, Fig. 3 represents the coverage probability versus the tilt angle for different values of β and λ_m in the noise limited regime. In this figure, the vertical line shows the optimal tilt angle obtained by lemma 2. As it is seen, the approximated tilt angle obtained in lemma 2 is very close to the optimal tilt angle. Also, these figures show that the coverage probability depends on the tilt angle and therefore by proper adjusting this angle by 3DBF, the performance can be improved.

Hereafter, we consider the coverage probability in the interference limited regime. Fig. 4 represents the effect of height on the optimal tilt angle for $\lambda_m = 10^{-4}$, $\beta = 0.03$. In this figure, we set $a = 1$ in (45), which means that the typical user is located at the height of h_0 . As it is seen, different user height will result in different optimal tilt angle. This shows the importance of considering the user height distribution on the tilt angle optimization. Notice that by network densification, the average radius of each cell decreases and the optimal

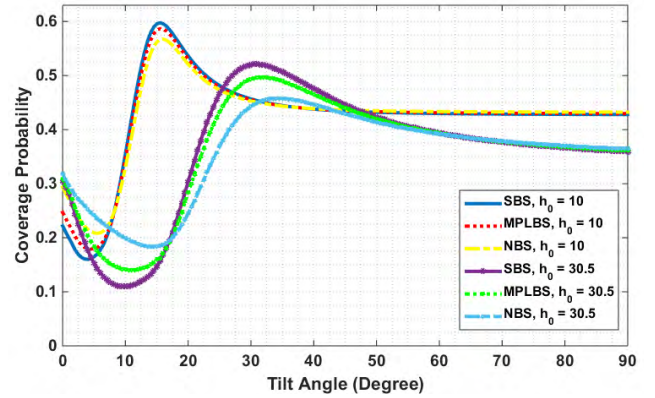


FIGURE 4. Coverage probability versus tilt angle for different h_0 (with $\lambda_m = 10^{-4}$, $\beta = 0.03$, $m = 1$ and $\tau = 5$ dB).

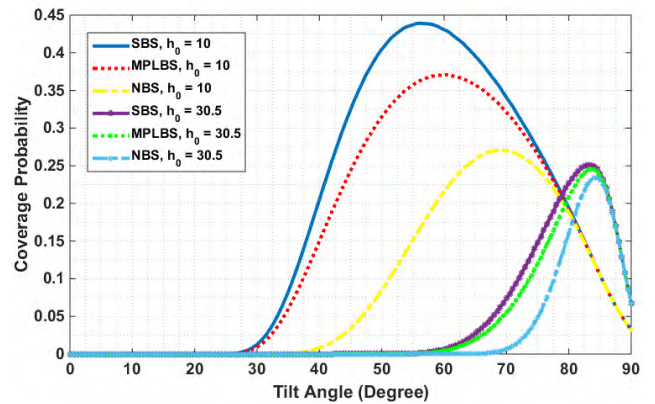


FIGURE 5. Coverage probability versus the tilt angle for different h_0 (with $\lambda_m = 10^{-2}$, $\beta = 0.003$, $m = 5$ and $\tau = 0$ dB).

tilt angle increases. Due to small average cell size in this case, a few variation in the tilt angle results in a significant performance degradation.

Fig. 5 represents the effect of users height on the optimal tilt angle for $\lambda_m = 10^{-2}$, $\beta = 0.003$. In this figure $a = 0.5$, which means that each user in 50 percent of the times is located at height of h_0 . Again it is observed that considering the user height has a significant effect on the optimal tilt angle and by increasing h_0 , the optimal tilt angle increases. The reason is that the serving BS can direct its beam to the user by larger down tilting. Also, it is observed that by further densification of the network, the optimal tilt angle increases since the average cell sizes decreases and the serving BS needs to use a larger down tilt angle to achieve maximum coverage. To be more specific, considering (40) and the NBS user association rule (in this case $\bar{r} = \frac{1}{\sqrt{\pi\lambda_m}}$), we have $\theta_{\text{opt}} \approx \text{atan}(\sqrt{\pi\lambda_m}\bar{h})$. Hence, for large values of λ_m, \bar{h} , θ_{opt} tends to 90° . The same trend can be observed for the SBS and MPLBS.

Fig. 6 shows the effect of users height distribution on the coverage probability (determined by parameter a in (45)) versus the tilt angle for $\lambda_m = 10^{-4}$, $m = 5$, $\beta = 0.03$, $\tau = 0$ dB

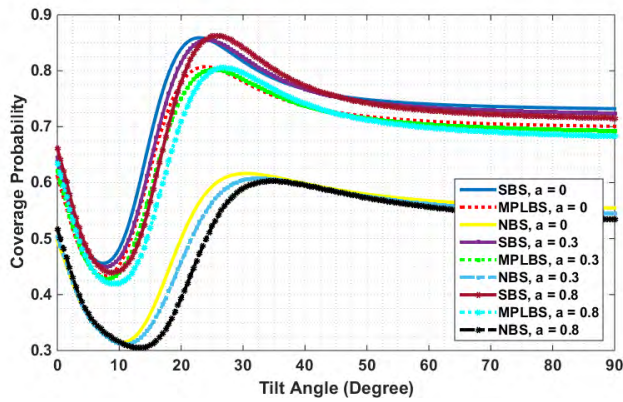


FIGURE 6. Coverage probability versus the tilt angle for different values of the parameter a (with $\lambda_m = 10^{-4}$, $\beta = 0.03$, $m = 5$ and $\tau = 0$ dB, $h_0 = 30.5$).

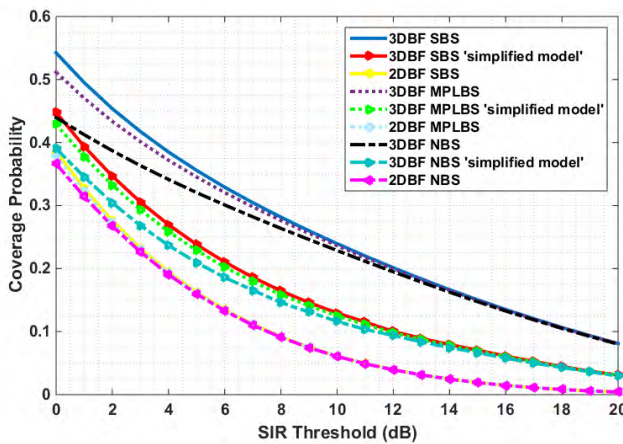


FIGURE 7. Coverage probability versus the SIR threshold and comparison of the 3DBF, 2DBF and the 'simplified model' (with $\lambda_m = 10^{-4}$, $\beta = 0.003$, $m = 5$, $a = 0.8$ and $h_0 = 10$).

and $h_0 = 30.5$. It is observed that by increasing the parameter a , i.e., the percent of the time that user is located at the fixed effective height h_0 , the total height behavior converges to the case that the user is located at this height. Since in this figure $h_0 = 30.5$ the optimal tilt angle slightly increases by increasing the parameter a . On the contrary, if $h_0 = 10$ then increasing the parameter a results in a decrease of the optimal tilt angle.

Fig. 7 illustrates the coverage probability versus the tilt angle for $\lambda_m = 10^{-4}$, $m = 5$, $\beta = 0.003$, $a = 0.8$ and $h_0 = 10$. This figure also compares 2DBF and 3DBF and a 'simplified model' for three different user association rules. By the 'simplified model', we mean the case that the user height distribution is ignored (user is located at $h_0 = 30.5$) which is usually assumed in the literature. It is seen that using 3DBF in the mmWave networks results in a significant performance improvement. Also, it is seen that ignoring the user height distribution, i.e., the 'simplified model', results in a significant degradation in the performance of the system.

Fig. 8 illustrates the boundaries given by the proposed low complexity approach in (38) and (39) by considering

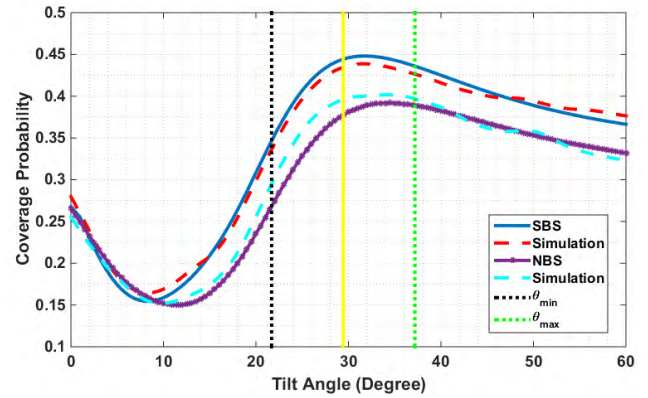


FIGURE 8. Coverage probability versus the tilt angle and illustration of the boundaries of the proposed low complexity approach (with $\lambda_m = 10^{-4}$, $\beta = 0.03$, $m = 1$, $a = 0.5$ and $h_0 = 30.5$).

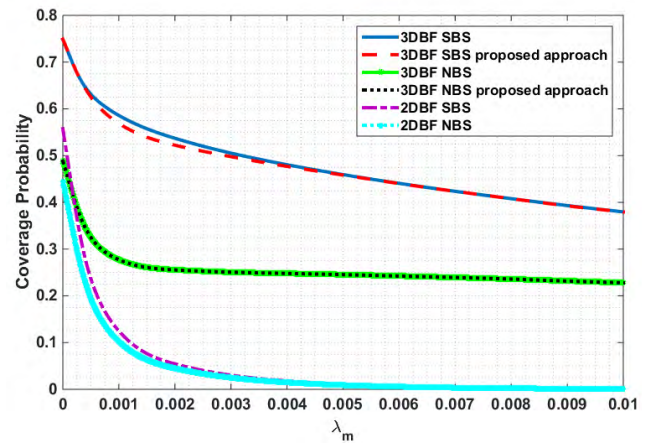


FIGURE 9. Coverage probability versus the base station density and comparison of the 3DBF, 2DBF and the proposed low complexity approach (with $\tau = 0$ dB, $\beta = 0.003$, $m = 1$, $a = 0.2$ and $h_0 = 10$).

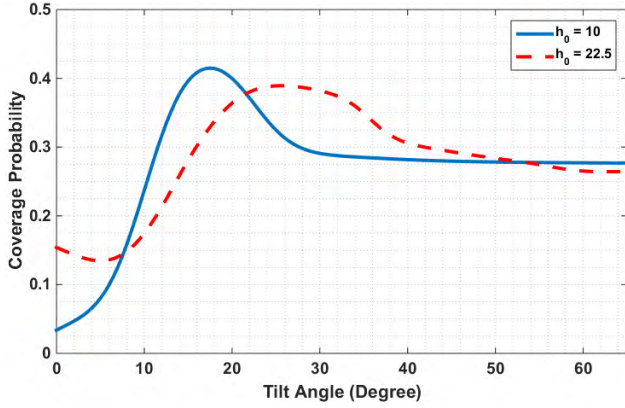
the SBS and NBS user association rules for $\lambda_m = 10^{-4}$, $m = 1$, $\beta = 0.03$, $a = 0.5$ and $h_0 = 30.5$. As it can be seen from the figure, the optimal value of the tilt angle is within the calculated boundaries. The vertical solid line is the approximated optimal tilt angle value in (40) which is very close to the optimal tilt angle.

Fig. 9 also represents the effect of 3DBF on the performance of the mmWave system in terms of λ_m with $m = 1$, $\tau = 0$ dB, $\beta = 0.003$, $a = 0.2$ and $h_0 = 10$. It is seen that the performance of the proposed low complexity approach is very close to the optimal value resulted from the exhaustive search.

Finally for evaluating the effect of the tilt angle on the coverage probability in a more realistic scenario, we adopt the channel model introduced in [32]. We consider the Uma channel model which is suitable for urban outdoor to outdoor communication in mmWave frequency bands and takes the users height parameter into account. The path loss equations for LOS and NLOS links are extracted from [32, table 7.4.1-1] and also, probability of the LOS link is given in [32, table 7.4.2-1]. The remaining channel model parameters are inherited from [32, section 7.5]. Simulation

TABLE 1. 3GPP simulation parameters.

Parameter	Value
BS height (H_{BS})	25 m
Users height (H_u)	2.5, 15 m
Shadow fading std [dB] (σ_{SF})	4 dB for LOS and 6 dB for NLOS
Number of clusters N	12
Number of rays per cluster M	20

**FIGURE 10.** Coverage probability versus tilt angle by considering the 3GPP model [32] (with $\tau = 0$ dB, $\alpha = 1$, $\lambda_m = 10^{-4}$).

parameters are given at table 1. Fig. 10 shows the results for $\alpha = 1$, $\lambda_m = 10^{-4}$. It is observed that the coverage probability in this setup has the same trend as the model we considered in our analyses.

VI. CONCLUSION

In this paper, we have studied the effect of the users height distribution on the coverage of mmWave cellular networks that utilize three dimensional beamforming (3DBF). It was assumed that the BSs and users are equipped with multiple antennas and LOS and NLOS links are modeled by Nakagami- m and Rayleigh fading, respectively. In this setup, we considered the tilt angle optimization to maximize the coverage probability for the noise limited and interference limited regimes. In the noise limited regime, we showed that the optimal tilt angle depends on the average distance of each user to its serving BS and also its *effective height*. Also, in the interference limited regime, we considered three different user association rules namely the nearest BS, minimum path loss BS and the strongest BS. Due to complexity of finding the optimal tilt angle in this regime, we proposed a low complexity approach. Through numerical results, we showed that the proposed low complex approach has performance close to the optimal solution found by the exhaustive search. Also, in this regime, we analyzed the behavior of the coverage probability in some asymptotic scenarios, e.g., where the BS density tends to infinity or zero and also where the SIR threshold tends to infinity or zero. Finally, using numerical results, we showed that adopting 3DBF in the mmWave networks and also including the users height distribution in the tilt angle optimization problem, result in a significant improvement in the performance of the network, for example, the optimal tilt angle improves the coverage probability by

a factor of three compared to the case that tilt angle is not optimized.

APPENDIX A

Proof: Proof of theorem 1: By definition of the coverage probability, we have

$$P_{C^I} = \Pr \{SIR > \tau\} = \int_0^\infty \int_{D_h} \Pr \left\{ |g_0|^2 L(r, h) > \frac{\tau I}{G(\theta_{\text{tilt}}, r, h)} \middle| x_0 = r, h_{\text{eff}} = h \right\} f_{h_{\text{eff}}}(h) f_R^{NB}(r) dh dr, \quad (46)$$

where

$$\Pr \left\{ |g_0|^2 L(r, h) > \frac{\tau I}{G(\theta_{\text{tilt}}, r, h)} \middle| x_0 = r, h_{\text{eff}} = h \right\} = E_I \{ \bar{F}_L(s_L I) \} P_L(r) + E_I \{ \bar{F}_N(s_N I) \} P_N(r). \quad (47)$$

Also, we have

$$\begin{aligned} E_I \{ \bar{F}_L(s_L I) \} &= E_I \left\{ e^{-ms_L I} \sum_{k=0}^{m-1} \frac{(ms_L I)^k}{k!} \right\} \\ &= \sum_{k=0}^{m-1} \frac{(ms_L)^k}{k!} E_I \left\{ e^{-ms_L I} (I)^k \right\} \\ &= \sum_{k=0}^{m-1} \frac{(-ms_L)^k}{k!} \left[\frac{d^k}{dz^k} \mathcal{L}_I(z) \right]_{z=ms_L}, \quad (48) \end{aligned}$$

where $\mathcal{L}_I(z) = E_I \{ \exp(-zI) \}$. In addition, we can divide the homogeneous PPP Φ into two non-homogeneous PPP, Φ_L and Φ_N with densities $\lambda_L(x_\ell) = \lambda_m P_L(x_\ell)$ and $\lambda_N(x_\ell) = \lambda_m P_N(x_\ell)$, respectively. Since Φ_L and Φ_N are independent, we have $\mathcal{L}_I(z) = \mathcal{L}_{I_L}(z) \mathcal{L}_{I_N}(z)$. In the following we calculate $\mathcal{L}_{I_L}(z)$ as

$$\begin{aligned} \mathcal{L}_{I_L}(z) &= E \left\{ \exp \left(-z \sum_{\substack{\ell: X_\ell \in \Phi_L, \\ \ell \neq 0}} |g_\ell|^2 \Lambda^2(Z_r^{0,\ell}) \right. \right. \\ &\quad \left. \left. \times G(\theta_{\text{tilt}}, x_\ell, h) (x_\ell^2 + h^2)^{-\alpha_L/2} \Lambda^2(Z_t^{\ell,\ell'}) \right) \right\} \\ &= E \left\{ \prod_{\substack{\ell: X_\ell \in \Phi, \\ \ell \neq 0}} \exp \left(-z |g_\ell|^2 \Lambda^2(Z_r^{0,\ell}) \right. \right. \\ &\quad \left. \left. \times G(\theta_{\text{tilt}}, x_\ell, h) (x_\ell^2 + h^2)^{-\alpha_L/2} \Lambda^2(Z_t^{\ell,\ell'}) \right) \right\} \\ &= E \left\{ \prod_{\substack{\ell: X_\ell \in \Phi_L, \\ \ell \neq 0}} E_{Z_t, Z_r} \{ K_L(Z_t, Z_r, m, \theta_{\text{tilt}}, x_\ell, h) \} \right\} \\ &= \exp \left(-2\pi \lambda_m \int_r^\infty \left(1 - E_{Z_t, Z_r} \{ K_L(Z_t, Z_r, m, \theta_{\text{tilt}}, x, h) \} \right) x P_L(x) dx \right). \quad (49) \end{aligned}$$

where the last equality comes from the probability generating functional (PGFL) of the PPP [29]. Similarly, we can calculate $\mathcal{L}_{I_N}(z)$ as

$$\mathcal{L}_{I_N}(z) = \exp \left(-2\pi\lambda_m \int_r^\infty \left(1 - E_{Z_t, Z_r} \{K_N(Z_t, Z_r, 1, \theta_{\text{tilt}}, x, h)\} \right) x P_N(x) dx \right). \quad (50)$$

Also notice that $E_I \{\bar{F}_N(s_N I)\} = \mathcal{L}_I(s_N)$. ■

APPENDIX B

Proof: Proof of theorem 3: Using the definition of the coverage probability we have

$$\begin{aligned} P_{C^I} &= \Pr(\cup_{x \in \Phi} \text{SIR}_x > \tau) = E \left\{ \sum_{x \in \Phi} \mathbb{1}_{\{\text{SIR}_x > \tau\}} \right\} \\ &\stackrel{(a)}{=} 2\pi\lambda_m \int_0^\infty \int_{D_h} \Pr \left\{ |g_0|^2 L(r, h) \right. \\ &\quad \left. > \frac{\tau I}{G(\phi_{\text{tilt}}, r, h)} \middle| x_0 = r, h_{\text{eff}} = h \right\} f_{h_{\text{eff}}}(h) r dh dr, \end{aligned} \quad (51)$$

where (a) comes from the Campbell theorem [29]. With similar steps taken as in (47), we can calculate the inner probability and derive the Laplace transform of the interference. In this case, the Laplace transform is

$$\begin{aligned} \mathcal{L}_{I_L}(z) &= E \left\{ \exp \left(-z \sum_{\ell: X_\ell \in \Phi_L} |g_\ell|^2 \Lambda^2(Z_r^{0, \ell}) \right. \right. \\ &\quad \left. \left. \times G(\theta_{\text{tilt}}, x_\ell, h) (x_\ell^2 + h^2)^{-\alpha_L/2} \Lambda^2(Z_t^{\ell, \ell'}) \right) \right\} \\ &= \exp \left(-2\pi\lambda_m \int_0^\infty \left(1 - E_{Z_t, Z_r} \{K_L(Z_t, Z_r, m, \theta_{\text{tilt}}, x, h)\} \right) x P_L(x) dx \right). \end{aligned} \quad (52)$$

APPENDIX C

Proof: Proof of lemma 5: As mentioned before, in the case that $\lambda_m \rightarrow \infty$, $P_{C^I} \sim P_c^L$ in which all the interfering BSs assumed to have LOS connection with the typical user. Thus, in this case we have

$$\begin{aligned} P_c^L &= E_{h,r} \left\{ \sum_{k=0}^{m-1} \frac{(-z)^k}{k!} \frac{d^k}{dz^k} \mathcal{L}_{I_L}(z) \middle|_{z=ms_L} \right\} \\ &\stackrel{(a)}{\leq} E_{h,r} \left\{ \sum_{n=1}^m (-1)^{n-1} \binom{m}{n} \mathcal{L}_{I_L}(c_n z) \middle|_{z=ms_L} \right\} \\ &\leq E_{h,r} \left\{ \sum_{n=1}^m \frac{1 - (-1)^n}{2} \binom{m}{n} \mathcal{L}_{I_L}(c_n z) \right\}, \end{aligned} \quad (53)$$

where $z = \frac{m\tau}{G(\theta, x, h)} (r^2 + h^2)^{\frac{\alpha_L}{2}}$, $c_n = n(\Gamma(m+1))^{\frac{-1}{m}}$ and $\mathcal{L}_{I_L}(z)$ given by (49) and (36) for nearest and strongest BS user association rules with $P_L(r) = 1$, respectively. Also, (a) is the result of the Alzer's inequality [33] and the last inequality is concluded from considering only positive terms. Therefore, it is sufficient to prove that $\lim_{\lambda_m \rightarrow \infty} \mathcal{L}_{I_L}(c_n z) = 0$ for the NBS user association rule. Furthermore, a similar approach can be used for the SBS user association rule. For the NBS user association rule we have (54), as shown at the top of the next page, where ${}_2F_1(\alpha, \beta; \gamma; z)$ denotes the Gauss hypergeometric function [34] and we define $b = E_{Z_t, Z_r} \left\{ {}_2F_1 \left(m, -\frac{2}{\alpha_L}; 1 - \frac{2}{\alpha_L}; -n\tau G_{\min} \Lambda^2(Z_r) \Lambda^2(Z_t) \right) \right\}$. Finally we notice that

$$\begin{aligned} \lim_{\lambda_m \rightarrow \infty} E_h \left\{ e^{-\pi\lambda_m(b-1)h^2} \right\} &= \lim_{\lambda_m \rightarrow \infty} \int_{D_h} e^{-\pi\lambda_m(b-1)h^2} f_{h_{\text{eff}}}(h) dh \\ &\leq \lim_{\lambda_m \rightarrow \infty} \frac{1}{\pi\lambda_m(b-1)} \int_{D_h} \frac{f_{h_{\text{eff}}}(h)}{h^2} dh \\ &\leq \lim_{\lambda_m \rightarrow \infty} \frac{1}{\pi\lambda_m(b-1)} \int_{D_h} f_{h_{\text{eff}}}(h) dh = 0. \end{aligned} \quad (55)$$

APPENDIX D

Proof: Using (41) we have

$$\begin{aligned} E \left\{ \exp \left(-2\pi C_1 \lambda_m \int_r^\infty \frac{xdx}{1 + \frac{G(\theta, r, h)}{\tau(r^2 + h^2)^{\frac{\alpha_N}{2}} G(\theta, x, h)} (x^2 + h^2)^{\frac{\alpha_N}{2}}} \right) \right\} \\ \geq E \left\{ \exp \left(-2\pi C_1 \lambda_m (r^2 + h^2) \left({}_2F_1 \left(1, -\frac{2}{\alpha_N}; 1 - \frac{2}{\alpha_N}, -\frac{\tau}{G(r, h, \theta)} \right) - 1 \right) \right) \right\} \\ \approx E \left\{ \exp \left(-2\pi C_1 \lambda_m (r^2 + h^2) \left(\frac{4\tau}{\alpha_N - 2} \frac{1}{G(\theta, r, h)} \right) \right) \right\} \\ \approx 1 - \frac{4\pi C_1 \lambda_m}{\alpha_N - 2} E_{h,r} \left\{ (r^2 + h^2) G^{-1}(\theta, r, h) \right\} \tau, \end{aligned} \quad (56)$$

where we use the well known approximation ${}_2F_1(\alpha, \beta; \gamma; z) \approx 1 + \frac{\alpha\beta}{\gamma}z$ for small values of z . For the SBS user association rule, using (42) we have

$$\begin{aligned} P_{C^I}^{SBS} &\geq E_{h,r} \left\{ \exp \left(-2\pi C_1 \lambda_m (r^2 + h^2) \int_0^\infty \frac{xdx}{1 + \frac{G(\theta, r, h)}{\tau G_{\min}} t^{\alpha_N}} \right) \right\} \\ &= E_{h,r} \left\{ \exp \left(-2\pi C_1 \lambda_m \int_0^\infty \frac{\left(\frac{\tau G_{\min}}{G(\theta, r, h)} \right)^{\frac{2}{\alpha_N}} x^{\frac{2}{\alpha_N} - 1}}{1 + x} \right) \right\} \end{aligned}$$

$$\begin{aligned}
E_{h,r} \{ \mathcal{L}_{L_L}(z) \} &\leq E_{h,r} \left\{ \exp \left(-2\pi\lambda_m E \left\{ \int_r^\infty \left(1 - \frac{1}{\left(1 + \frac{n\tau G_{\min}}{m} \Lambda^2 \left(Z_r^{0,\ell} \right) (x^2 + h^2)^{-\frac{\alpha_L}{2}} \Lambda^2 \left(Z_t^{\ell,\ell'} \right) \right)^m} \right) x dx \right\} \right) \right\} \\
&= E_{h,r} \left\{ \exp \left(-2\pi\lambda_m E \left\{ \int_{\sqrt{r^2+h^2}}^\infty \left(1 - \frac{1}{\left(1 + \frac{n\tau G_{\min}}{m} \Lambda \left(Z_r^{0,\ell} \right) u^{-\alpha_L} \Lambda \left(Z_t^{\ell,\ell'} \right) \right)^m} \right) u du \right\} \right) \right\} \\
&\leq E_{h,r} \left\{ \exp \left(-\pi\lambda_m (r^2 + h^2) E \left\{ {}_2F_1 \left(m, -\frac{2}{\alpha_L}; 1 - \frac{2}{\alpha_L}; -n\tau G_{\min} \Lambda^2 \left(Z_r^{0,\ell} \right) \Lambda^2 \left(Z_t^{\ell,\ell'} \right) \right) - 1 \right\} \right) \right\} \\
&= E_h \left\{ \frac{1}{2\pi\lambda_m b} e^{-\pi\lambda_m (b-1)h^2} \right\}, \tag{54}
\end{aligned}$$

$$\begin{aligned}
&\stackrel{(a)}{=} E_{h,r} \left\{ \exp \left(-2\pi C_1 \lambda_m \frac{\pi}{\sin \left(\frac{2\pi}{\alpha_N} \right)} (r^2 + h^2) \left(\frac{\tau G_{\min}}{G(\theta, r, h)} \right)^{\frac{2}{\alpha_N}} \right) \right\} \\
&\approx 1 - \frac{2\pi^2 C_1 \lambda_m}{\sin \left(\frac{2\pi}{\alpha_N} \right)} E_{h,r} \left\{ \frac{r^2 + h^2}{G^{\frac{2}{\alpha_N}}(\theta, r, h)} \right\} \tau^{\frac{2}{\alpha_N}}, \tag{57}
\end{aligned}$$

where (a) is deduced from the definition of the beta function and the fact that $B(x, 1-x) = \frac{\pi}{\sin(x\pi)}$. ■

APPENDIX E

Proof: In this case for the SBS user association rule using (41) we have

$$\begin{aligned}
&E \left\{ \exp \left(-2\pi C_1 \lambda_m \int_r^\infty \frac{xdx}{1 + \frac{G(\theta, r, h)}{\tau(r^2+h^2)^{\frac{\alpha_N}{2}} G(\theta, x, h)} (x^2 + h^2)^{\frac{\alpha_N}{2}}} \right) \right\} \\
&\leq E_{h,r} \left\{ \exp \left(-2\pi C_1 \lambda_m (r^2 + h^2) \times \left({}_2F_1 \left(1, -\frac{2}{\alpha_N}; 1 - \frac{2}{\alpha_N}, -\frac{\tau G_{\min}}{G(r, h, \theta)} \right) - 1 \right) \right) \right\} \\
&\stackrel{(a)}{=} E_{h,r} \left\{ \exp \left(-2\pi C_1 \lambda_m (r^2 + h^2) \left(\left(1 + \frac{\tau G_{\min}}{G(r, h, \theta)} \right)^{\frac{2}{\alpha_N}} \times {}_2F_1 \left(-\frac{2}{\alpha_N}, -\frac{2}{\alpha_N}; 1 - \frac{2}{\alpha_N}, \frac{\tau G_{\min}}{G(r, h, \theta)} \right) - 1 \right) \right) \right\} \\
&\stackrel{(b)}{\approx} E_{h,r} \left\{ \exp \left(-\pi C_1 \lambda_m (r^2 + h^2) \frac{C_2 G_{\min}^{\frac{2}{\alpha_N}} \tau^{\frac{2}{\alpha_N}}}{G(r, h, \theta)^{\frac{2}{\alpha_N}}} \right) \right\}
\end{aligned}$$

$$\begin{aligned}
&\leq E_{h,r} \left\{ \exp \left(-\pi C_1 \lambda_m (r^2 + h^2) C_0 G_{\min}^{\frac{2}{\alpha_N}} \tau^{\frac{2}{\alpha_N}} \right) \right\} \\
&= \frac{G_{\min}^{-\frac{2}{\alpha_N}}}{C_2} E_h \left\{ e^{-\pi C_1 \lambda_m h^2 C_2 G_{\min}^{\frac{2}{\alpha_N}} \tau^{\frac{2}{\alpha_N}}} \right\} \tau^{-\frac{2}{\alpha_N}} \\
&\leq \frac{G_{\min}^{-\frac{4}{\alpha_N}}}{C_2^2} E_h \left\{ \frac{1}{\pi C_1 \lambda_m h^2} \right\} \tau^{-\frac{4}{\alpha_N}}, \tag{58}
\end{aligned}$$

where (a) comes from the fact that ${}_2F_1(\alpha, \beta; \gamma; z) = (1-z)^{-\beta} {}_2F_1(\beta, \gamma-\alpha; \gamma; \frac{z}{z-1})$, and (b) result from $1 + \frac{G_{\min}\tau}{G(r, h, \theta)} \approx \frac{G_{\min}\tau}{G(r, h, \theta)}$, $\frac{G_{\min}\tau}{1 + \frac{G_{\min}\tau}{G(r, h, \theta)}} \approx 1$ for $\tau \rightarrow \infty$ and the fact

that ${}_2F_1(\alpha, \beta; \gamma; 1) = \frac{\Gamma(\gamma)\Gamma(\gamma-\alpha-\beta)}{\Gamma(\gamma-\alpha)\Gamma(\gamma-\beta)}$. Also, in this case for the SBS user association rule from (42) we have

$$\begin{aligned}
P_{C_I}^{NSB} &\leq E_{h,r} \left\{ \exp \left(-\frac{2\pi^2 C_1 \lambda_m}{\sin \left(\frac{2\pi}{\alpha_N} \right)} (r^2 + h^2) \tau^{\frac{2}{\alpha_N}} \right) \right\} \\
&= E_h \left\{ e^{-\frac{2\pi^2 C_1 \lambda_m}{\sin \left(\frac{2\pi}{\alpha_N} \right)} \tau^{\frac{2}{\alpha_N}} h^2} \right\} \frac{\sin \left(\frac{2\pi}{\alpha_N} \right)}{\pi} \tau^{-\frac{2}{\alpha_N}} \\
&\leq \frac{\sin \left(\frac{2\pi}{\alpha_N} \right)^2}{2\pi^3 C_1 \lambda_m} E_h \left\{ \frac{1}{h^2} \right\} \tau^{-\frac{4}{\alpha_N}}. \tag{59}
\end{aligned}$$

REFERENCES

- [1] F. Al-Turjman, E. Ever, and H. Zahmatkesh, "Small cells in the forthcoming 5G/IoT: Traffic modelling and deployment overview," *IEEE Commun. Surv. Tuts.*, vol. 21, no. 1, pp. 28–65, 1st Quart., 2019.
- [2] J. G. Andrews et al., "What will 5G be?" *IEEE J. Sel. Areas Commun.*, vol. 32, no. 6, pp. 1065–1082, Jun. 2014.
- [3] S. M. Razavizadeh, M. Ahn, and I. Lee, "Three-dimensional beamforming: A new enabling technology for 5G wireless networks," *IEEE Signal Process. Mag.*, vol. 31, no. 6, pp. 94–101, Nov. 2014.

- [4] Q. U. A. Nadeem, A. Kammoun, and M. Alouini, "Elevation beamforming with full dimension MIMO architectures in 5G systems: A tutorial," 2018, *arXiv:1805.00225*. [Online]. Available: <https://arxiv.org/abs/1805.00225>
- [5] N. Seifi, R. W. Heath, Jr., M. Coldrey, and T. Svensson, "Adaptive multicell 3-D beamforming in multi-antenna cellular networks," *IEEE Trans. Veh. Technol.*, vol. 65, no. 8, pp. 6217–6231, Aug. 2016.
- [6] N. Seifi, J. Zhang, R. W. Heath, Jr., T. Svensson, and M. Coldrey, "Coordinated 3D beamforming for interference management in cellular networks," *IEEE Trans. Wireless Commun.*, vol. 13, no. 10, pp. 5396–5410, Oct. 2014.
- [7] W. Lee, S.-R. Lee, H.-B. Kong, S. Lee, and I. Lee, "Downlink vertical beamforming designs for active antenna systems," *IEEE Trans. Commun.*, vol. 62, no. 6, pp. 1897–1907, Jun. 2014.
- [8] O. G. Aliu, A. Imran, M. A. Imran, and B. Evans, "A survey of self organisation in future cellular networks," *IEEE Commun. Surveys Tuts.*, vol. 15, no. 1, pp. 336–361, 2nd Quart., 2013.
- [9] R. Hernandez-Aquino, S. A. R. Zaidi, D. McLernon, M. Ghogho, and A. Imran, "Tilt angle optimization in two-tier cellular networks—A stochastic geometry approach," *IEEE Trans. Commun.*, vol. 63, no. 12, pp. 5162–5177, Dec. 2015.
- [10] Y. Khan, B. Sayrac, and E. Moulines, "Active antenna systems for centralized self-optimization of capacity in LTE-A," in *Proc. IEEE Wireless Commun. Netw. Conf. Workshops (WCNCW)*, Apr. 2014, pp. 166–171.
- [11] T. S. Rappaport et al., "Millimeter wave mobile communications for 5G cellular: It will work!" *IEEE Access*, vol. 1, pp. 335–349, May 2013.
- [12] L. Wei, R. Q. Hu, Y. Qian, and G. Wu, "Key elements to enable millimeter wave communications for 5G wireless systems," *IEEE Wireless Commun.*, vol. 21, no. 6, pp. 136–143, Dec. 2014.
- [13] J. G. Andrews, F. Baccelli, and R. K. Ganti, "A tractable approach to coverage and rate in cellular networks," *IEEE Trans. Commun.*, vol. 59, no. 11, pp. 3122–3134, Nov. 2011.
- [14] T. Bai and R. W. Heath, Jr., "Coverage and rate analysis for millimeter-wave cellular networks," *IEEE Trans. Wireless Commun.*, vol. 14, no. 2, pp. 1100–1114, Feb. 2015.
- [15] H. ElSawy, A. Sultan-Salem, M. S. Alouini, and M. Z. Win, "Modeling and analysis of cellular networks using stochastic geometry: A tutorial," *IEEE Commun. Surveys Tuts.*, vol. 19, no. 1, pp. 167–203, 1st Quart., 2017.
- [16] A. H. Jafari, D. López-Pérez, M. Ding, and J. Zhang, "Performance analysis of dense small cell networks with practical antenna heights under Rician fading," *IEEE Access*, vol. 6, pp. 9960–9974, 2018.
- [17] M. Gapeyenko et al., "On the temporal effects of mobile blockers in urban millimeter-wave cellular scenarios," *IEEE Trans. Veh. Technol.*, vol. 66, no. 11, pp. 10124–10138, Nov. 2017.
- [18] I. Atzeni, J. Arnau, and M. Kountouris, "Downlink cellular network analysis with LOS/NLOS propagation and elevated base stations," *IEEE Trans. Wireless Commun.*, vol. 17, no. 1, pp. 142–156, Jan. 2018.
- [19] P. Chandhar and S. S. Das, "Multi-objective framework for dynamic optimization of OFDMA cellular systems," *IEEE Access*, vol. 4, pp. 1889–1914, 2016.
- [20] N. Seifi, M. Coldrey, and M. Viberg, "Throughput optimization for MISO interference channels via coordinated user-specific tilting," *IEEE Commun. Lett.*, vol. 16, no. 8, pp. 1248–1251, Aug. 2012.
- [21] S. K. Moghaddam and S. M. Razavizadeh, "Joint tilt angle adaptation and beamforming in multicell multiuser cellular networks," *Comput. Elect. Eng.*, vol. 61, pp. 195–207, Jul. 2017.
- [22] M. Baianifar, S. Khavari, S. M. Razavizadeh, and T. Svensson, "Impact of user height on the coverage of 3D beamforming-enabled massive MIMO systems," in *Proc. IEEE 28th Annu. Int. Symp. Pers., Indoor, Mobile Radio Commun. (PIMRC)*, Oct. 2017, pp. 1–5.
- [23] J. Yang, M. Ding, G. Mao, Z. Lin, D. Zhang, and T. H. Luan, "Optimal base station antenna downtilt in downlink cellular networks," 2018, *arXiv:1802.07479*. [Online]. Available: <https://arxiv.org/abs/1802.07479>
- [24] M. Baianifar, S. M. Razavizadeh, H. Akhlaghpasand, and I. Lee, "Energy efficiency maximization in mmWave wireless networks with 3D beamforming," *J. Commun. Netw.*, vol. 21, no. 2, pp. 125–135, Apr. 2019.
- [25] M. Haenggi and R. K. Ganti, "Interference in large wireless networks," *Found. Trends Netw.*, vol. 3, no. 2, pp. 127–248, 2009.
- [26] Q.-U.-A. Nadeem, A. Kammoun, M. Debbah, and M.-S. Alouini, "Performance analysis of compact FD-MIMO antenna arrays in a correlated environment," *IEEE Access*, vol. 5, pp. 4163–4178, 2017.
- [27] Q.-U.-A. Nadeem, A. Kammoun, M. Debbah, and M.-S. Alouini, "Design of 5G full dimension massive MIMO systems," *IEEE Trans. Commun.*, vol. 66, no. 2, pp. 726–740, Feb. 2018.
- [28] *Technical Specification Group Radio Access Network; Evolved Universal Terrestrial Radio Access (E-UTRA); Further Advancements for E-UTRA Physical Layer Aspects (Release9)*, document 3GPP TR 36.814 V9.0.0, Mar. 2010.
- [29] M. Haenggi, *Stochastic Geometry for Wireless Networks*. Cambridge, U.K.: Cambridge Univ. Press, Nov. 2012.
- [30] T. Bai, R. Vaze, and R. W. Heath, Jr., "Analysis of blockage effects on urban cellular networks," *IEEE Trans. Wireless Commun.*, vol. 13, no. 9, pp. 5070–5083, Sep. 2014.
- [31] F. Athley and M. N. Johansson, "Impact of electrical and mechanical antenna tilt on LTE downlink system performance," in *Proc. IEEE 71st Veh. Technol. Conf.*, May 2010, pp. 1–5.
- [32] *Study on Channel Model for Frequency Spectrum Above 6 GHz*, document 3GPP TR 38.900 V15.0.0, Jun. 2018.
- [33] H. Alzer, "On some inequalities for the incomplete gamma function," *Math. Comput.*, vol. 66, no. 218, pp. 771–778, Apr. 1997.
- [34] I. S. Gradshteyn, I. M. Ryzhik, and A. Jeffrey, *Table of Integrals, Series and Products*, 7th ed. Amsterdam, The Netherlands: Elsevier, 2007.



the stochastic geometry in wireless communications.

MAHDI BAIANIFAR received the B.Sc. degree in electrical engineering from the University of Zanjan, Iran, and the M.Sc. degree in electrical engineering from the Sharif University of Technology, Tehran, Iran, in 2011 and 2013, respectively. He is currently pursuing the Ph.D. degree with the Iran University of Science and Technology (IUST). His research interests include the area of wireless communication systems and specially in the area of mmWave networks, and application of



and also the head of the Communications Group. His research interest includes the area of signal processing for wireless communication systems. He is a senior member of IEEE.

S. MOHAMMAD RAZAVIZADEH received the B.Sc., M.Sc., and Ph.D. degrees in electrical engineering from the Iran University of Science and Technology (IUST), Tehran, Iran, in 1997, 2000, and 2006, respectively. From 2005 to 2011, he was with Iran Telecomm. Research Center as a Research Assistant Professor and also the Director of the Radio Communications Group. Since 2011, he has been with School of Electrical Engineering, IUST, where he is currently an Associate Professor



SOHEIL KHAVARI-MOGHADDAM received the B.Sc. degree in electrical engineering from the Amirkabir University of Technology (AUT), Tehran, Iran, in 2013, and the M.Sc. degree in electrical engineering from the Iran University of Science and Technology (IUST), Tehran, in 2016, where he is currently pursuing the Ph.D. degree with the School of Electrical Engineering. His current research interests include wireless communication and machine learning.



TOMMY SVENSSON (S'98–M'03–SM'10) received the Ph.D. degree in information theory from the Chalmers University of Technology, Gothenburg, Sweden, in 2003, where he is currently a Full Professor in communication systems, and also leading the Wireless Systems Research on air interface and wireless backhaul networking technologies for future wireless systems. He was with Ericsson AB with core networks, radio access networks, and microwave transmission products.

He was involved in the European WINNER and ARTIST4G projects that made important contributions to the 3GPP LTE standards, the EU FP7 METIS, and the EU H2020 5GPPP mmMAGIC 5G projects. He is involved in the EU H2020 5GPPP 5GCar Project. He is also with the ChaseOn Antenna Systems Excellence Center, Chalmers University of Technology, where he is involved in mm-wave solutions for 5G access, backhaul, and V2X scenarios. He has coauthored four books, 80 journal papers, 121 conference papers, and 51 public EU projects deliverables. His research interests include design and analysis of physical layer algorithms, multiple access, resource allocation, cooperative systems, moving networks, and satellite networks. He is the Chairman of the IEEE Sweden joint Vehicular Technology/Communications/Information Theory Societies chapter and an Editor of the IEEE TRANSACTIONS ON WIRELESS COMMUNICATIONS. He has been an Editor of the IEEE WIRELESS COMMUNICATIONS LETTERS and the Guest Editor of several top journals. He has organized several tutorials and workshops at top IEEE conferences and has served as a Coordinator for the Communication Engineering Master's Program at Chalmers University of Technology.

...